Integrated holographic filters for flat passband optical multiplexers

D. Iazikov, C. M. Greiner, and T. W. Mossberg

LightSmyth Technologies, 860 W. Park St. Suite 250
Eugene, Oregon 97401
twmoss@Lightsmyth.com

Abstract: Lithographically rendered, slab-waveguide-based, volume holographic filters are shown, via fabrication and test, capable of providing fully integrated, single-mode compatible, flat-topped and low loss filtering for wide bandwidth multiplexers as, for example, used in coarse wave-division multiplexing (CWDM). Single-mode compatibility is preserved since the filters operate via multi-path interference like thin-film filters rather than the angular dispersion typically utilized by grating type devices. Flexible apodization, entirely consistent with simple binary etch, is employed to provide steep passband falloff. High reflectivity and wide bandwidth is enabled through a tailored dual core waveguide geometry providing for mode concentration on the diffractive elements.

OCIS codes: (230.3120) Integrated optics devices; (230.7390) Waveguides, planar; (050.7330) Volume holographic gratings; (060.4230) Multiplexing

References

1. M. K. Smit, "New focusing and dispersive planar component based on an optical phased array," Electron. Lett. **24**, 385-386 (1988).
2. H. Takahashi, S. Suzuki, K. Kato, and I. Nishi, "Arrayed waveguide grating for wavelength division multi/demultiplexer with nanometer resolution," Electron. Lett. **26**, 87-88 (1990).
3. C. Dragone, "An N x N optical multiplexer using a planar arrangement of two star couplers," IEEE Photonics Technol. Lett. **3**, 812-815 (1991).
4. J. He, B. Lamontagne, A. Delage, L. Erickson, M. Davies, and E. S. Koteles, "Monolithic Integrated Wavelength Demultiplexer Based on a Waveguide Rowland Circle Grating in InGaAsP/InP," J. Lightwave. Technol. **16**, 631-638 (1998).
5. V. I. Tolstikhin, A. Densmore, K. Pimenov, Y. Logvin, F. Wu, S. Laframboise, and S. Grabtchak, "Monolithically Integrated Optical Channel Monitor for DWDM Transmission Systems," J. Lightwave Technol. **22**, 146-153 (2004).
6. W. R. Babbitt and T. W. Mossberg, "Optical waveform processing and routing with structured surface gratings," Opt. Commun. **148**, 23 (1998).
7. K. Okamoto and H. Yamada, "Arrayed-waveguide grating multiplexer with flat spectral response," Opt. Lett. **20**, 43-45 (1995).
8. C. R. Doerr, M. Cappuzzo, L. Gomez, E. Chen, A. Wong-Foy, C. Ho, J. Lam, and K. McGreer, "Planar Lightwave Circuit Eight-Channel CWDM Multiplexer with <3.9-dB Insertion Loss," J. Lightwave Technol. **23**, 62-65 (2005).
9. C. R. Doerr, R. Pafchek, and L. W. Stulz, "Integrated Band Demultiplexer Using Waveguide Grating Routers," IEEE Photonics Technol. Lett. **15**, 1088-1090 (2003).
10. T. W. Mossberg, "Planar holographic optical processing devices," Opt. Lett. **26**, 414-416 (2001).
11. C. H. Henry, R. F. Kazarinov, Y. Shani, R. C. Kistler, V. Pol, and K. J. Orlowsky, "Four-channel wavelength division multiplexers and bandpass filters based on elliptical Bragg reflectors," J. Lightwave Technol. **8**, 748-755 (1990).
12. D. Iazikov, C. Greiner, and T. W. Mossberg, "Apodizable Integrated Filters for Coarse WDM and FTTH-Type Applications," J. Lightwave Technol. **22**, 1402-1407 (2004).
13. T. W. Mossberg, C. Greiner, and D. Iazikov, "Interferometric Amplitude Apodization of Integrated Gratings," Opt. Express **13**, 2419 - 2426 (2005).

#10401 - $15.00 USD Received 23 January 2006; revised 31 March 2006; accepted 3 April 2006

1. Introduction

Frequency-selective optical elements are vital in all aspects of optical science and technology. This is particularly true in communications where filtering elements must selectively route or process frequency-differentiated optical data streams. There remains a need for flexible building-block filtering elements compatible with monolithic integration, general passband definition, and single-mode operation. In this publication, we describe the performance of innovative lithographically-scribed, integrated-holographic filtering elements and a flat-top multiplexer based thereon. The filtering elements demonstrated expand the range of integrated filtering performance available.

Integrated spectral filters in widespread use are based primarily on reflective or transmissive gratings, e. g. arrayed waveguide gratings [1-3], echelle gratings [4-5], etc. and these gratings function on the basis of angular dispersion. Angularly dispersive devices are very good at routing many signal channels with Gaussian-like passbands into separate output channels. But they have a fundamental limitation when it comes to mapping channels of complex passband (spanning a range of output directions) into single-mode (direction specific) outputs. Generally speaking, angularly dispersive filters can be configured to deliver tailored, e. g. flat top, passbands into single-mode outputs, but to do so requires an insertion loss (IL) penalty, which becomes more severe as the number of grating resolution bandwidths coupled to the output increases. [6-7] It has been shown that one can use double grating devices to more flexibly route tailored passbands into single-mode outputs. [8-9] In such cases, the second grating is employed to realign selected angularly dispersed signals into a common output direction. While adding a second grating provides substantially more passband flexibility, its addition carries with it the price of increased complexity and size.

Angular dispersion is not the only spectral filtering mechanism available. Thin film filters, for example, operate by a different principle, i. e. multipath interference. Passbands are defined through the interaction of unidirectional light with a series of dielectric interfaces. Quite general passbands can be achieved and routed to single-mode outputs without fundamental IL penalty. Thin-film filters combine device simplicity and compactness with single-mode function, but are not compatible with monolithic integration in their normal form.

The integrated holographic filtering devices described here can be described as gratings, but, being volume gratings, they function via multipath interference, like thin-film filters, and thus offer flexible passband control without IL penalty. Furthermore, the reflective interfaces of the integrated holographic filter, lithographically etched trenches, are curved so that they provide a focusing of signals between input and output ports as well as interferometrically defining the spectral passband. [10] We note that simpler geometrically based volume grating filters have also been described. [11] It should be noted that fiber Bragg gratings also function via multipath interference.

2. Device description

We have previously reported on the basic geometry of integrated holographic filters and multiplexers. [10,12] Early work suffered from defects in the apodization approach, which introduced artifacts into the intended passband and from high IL resulting from the low interfacial reflectivity available with standard slab waveguide geometries. In the present work, we describe a dual core waveguide geometry that provides sufficient interfacial reflectivity to create millimeter length filters with very low IL and passbands in excess of fifteen nanometers wide. Additionally, we implement a robust, binary-etch-compatible apodization approach free from the distorting effects previously reported. With the enhancements mentioned, planar holographic devices have reached performance levels competitive with discrete-film filters and moreover comprise a fully integrated technology.

Figure 1 gives a schematic view of a four-channel multiplexer based on integrated holographic filters. The top portion of the Fig. 1 looks down on a silica-on-silicon die.

#10401 - $15.00 USD Received 23 January 2006; revised 31 March 2006; accepted 3 April 2006

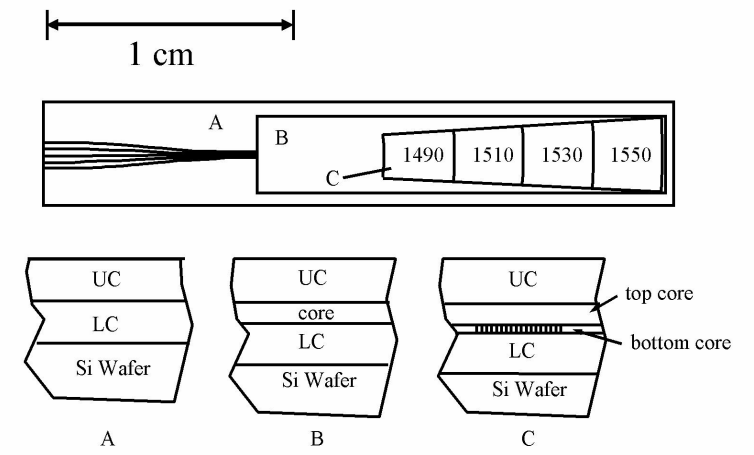

Fig. 1. Schematic top view of four-channel multiplexer chip with cross-section views of chip regions A, B and C.

The regions labeled A, B, and C have the respective cross sections shown at the bottom of Fig. 1. The lines on the left of the die view (top) represent channel waveguides coupling signals from the edge of the die to the slab waveguide regions B and C. Region A is non-guiding. The overall die dimensions are approximately 4 x 26 mm. Entering region B, the five channel waveguides have a total lateral spread of 250 microns, while at the edge of the die their lateral spread is 1 mm (250 micron channel-to-channel spacing). The central channel waveguide is common and in a demultiplexing implementation each of the four filters focuses signals emerging from the common channel and within its respective reflection passband to one of the outlaying four channels. The focusing action is reciprocal enabling multiplexing and demultiplexing function. In the cross-sectional views, the upper (UC) and lower (LC) cladding layers are, respectively, doped silica and thermal oxide. Both cladding layers have a thickness of ≈14 microns and a refractive index ≈1.45. The core region comprises a single (two) layer(s) and is approximately 2.3 (2.6) microns thick in region B (C). The upper (lower) core layer has a refractive index about 0.7 (4) percent above the cladding index. In all regions, only a single vertical spatial mode is supported. The filter structure is etched into the top of the lower core layer in region C using Deep Ultraviolet (DUV) reduction photolithography. The reticle is written via laserwriter on a scale four times the actual device dimensions. The diffractive contours comprising the volume holographic grating individually image a portion of the input signal to the output channel. In the present instance the imaging is 1:1, but there is no need for this and the contours can be general providing for optimal wavefront matching between ports. There are about 5400 diffractive contours in each ≈ 2.7-mm-long filter section.

Note that a lower, higher index, core layer is added in Region C. Diffractive contours are created by etch of the lower core and fill with upper core material. The region of diffractive contours has the highest average refractive index leading to an enhancement of the guided-mode field in the diffractive contour region and strong field-contour coupling. Strong field-contour coupling is required to achieve high reflectivity over bandwidths as large as those demonstrated here. The dual core approach allows for guided layers thick enough to couple effectively to fibers while simultaneously providing needed field-contour coupling. Serendipitously, control of the lower core properties is found to allow for a zeroing of polarization dependent wavelength shift by means which are not yet fully understood.

The integrated holographic filters fabricated are designed to meet the passband requirements of coarse wavelength-division multiplexing (CWDM), i.e. 13-nm wide, flat-top passbands with low IL. Such passbands are difficult to achieve at acceptable IL levels with current single-mode compatible, integrated filters. [8,9] To achieve such a wide passband, the average spacing of diffractive contours within a filter is chirped. The smallest spacing is

#10401 - $15.00 USD Received 23 January 2006; revised 31 March 2006; accepted 3 April 2006

located on the input side of the filter. Locally, the average spacing, Λ, of the diffractive contours is related to the vacuum wavelength of resonant backscattering, λ_b, according to $\lambda_b = 2n_e\Lambda$, where n_e is the local effective waveguide refractive index. To achieve rapid passband falloff in the wings, the reflective amplitude of the filter is apodized using a correlated-line apodization scheme. [13] The local value of λ_b and reflective amplitude as a function diffractive contour number (contour 1 is on the input side) is shown in Fig. 2. As described elsewhere, [13] correlated-line apodization provides for reflective amplitude control by spatial placement of small sets of diffractive contours so as to interferometrically set the net reflectivity of the set to desired values. This method allows for the use of standard binary (single depth) etch fabrication. The spacing between contours within the first filter is shown in Fig. 3. Amplitudes above 0.98 are treated as unity so that in the central region the spacing is a simple chirp.

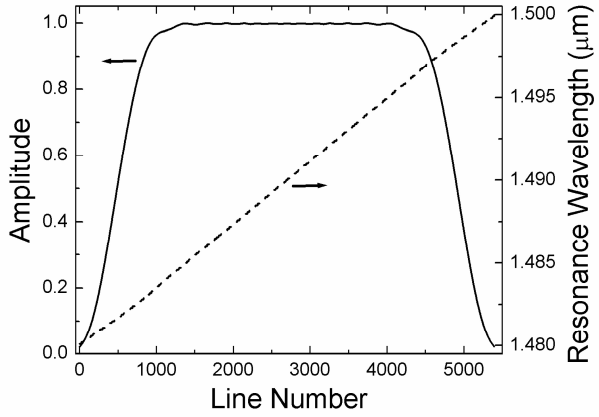

Fig. 2. Local reflective amplitude (solid line) and wavelength (dashed line) of integrated holographic filters as a function of contour number. Lower numbered contours are closest to the access waveguides.

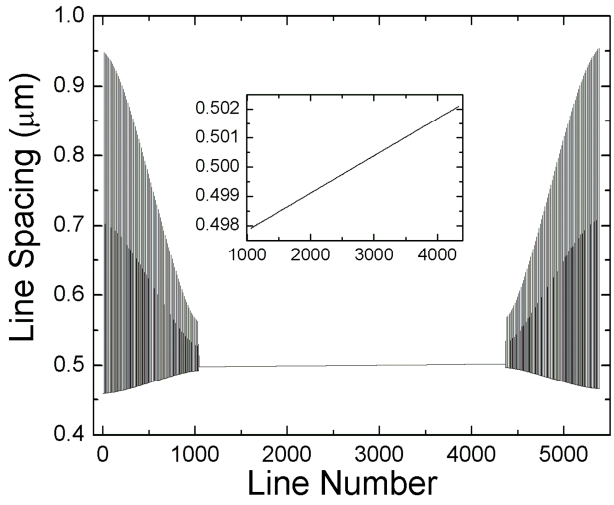

Fig. 3. Spacing between adjacent diffractive contours comprising the integrated holographic filters. Rapid variations for low and high contour numbers indicate contour displacements necessary to interferometrically apodize local reflective amplitude. Insert shows the central chirped region with increased vertical resolution.

#10401 - $15.00 USD Received 23 January 2006; revised 31 March 2006; accepted 3 April 2006

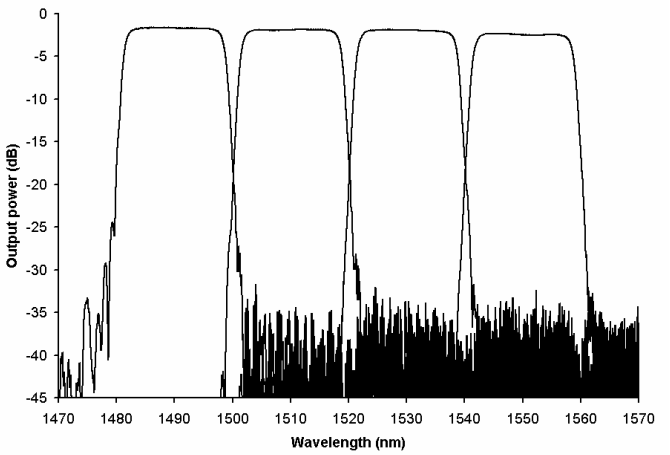

Fig. 4. Reflection passbands for each of the four channels comprising the apodized multiplexer/demultiplexer. Output power level shown includes all losses including fiber to die.

3. Measurements

The measured reflection spectrum of the each of the four integrated filters is shown in Fig. 4. Each passband is coupled to a separate output channel. The IL includes a 1.3 dB fiber-to-die coupling loss determined in separate measurements, which is consistent with refractive indices and channel waveguide dimensions. On-chip loss of the first channel (about 1.6 dB IL) is thus only about 0.3 dB. By the fourth channel, the IL has increased to approximately 2.4 dB. It is believed that on-chip loss comes from a combination of out-of-plane scattering introduced by the apodization method and from avoidable film inhomogeneities that interfere with focusing into the output channels. Both effects accumulate with total propagation length and hence channel number. The passband flatness is found to be better than 0.3 dB. Isolation between adjacent channels is better than 34 dB. Part of the observed channel-cross talk is attributed to scattering from variant designs closely spaced within the die (not shown in Fig. 1 and which would not exist in a dedicated device). Increases in the spacing of output channel waveguides (as they enter the slab region) are also expected to reduce crosstalk.

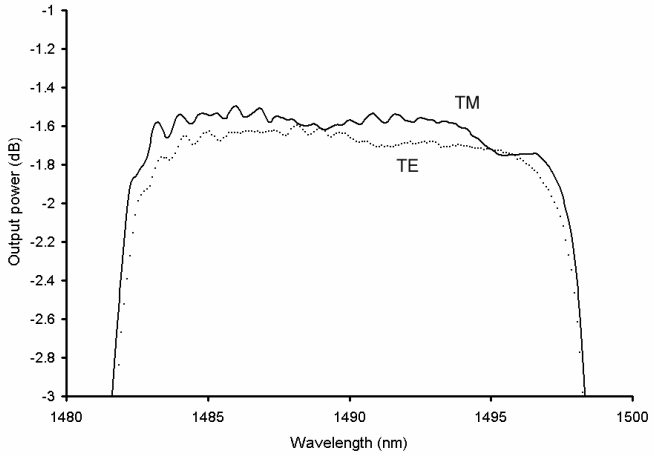

Fig. 5. An apodized filter passband shown on an expanded scale explicitly showing polarization dependence.

#10401 - $15.00 USD Received 23 January 2006; revised 31 March 2006; accepted 3 April 2006

Figure 5 shows an enlarged view of the first channel's passband with both polarizations shown. The polarization dependent loss, PDL, is less than 0.2 dB for all four channels. We believe that the low PDL comes from a combination of three factors: 1) All reflections are at near normal incidence, 2) The maximal index contrast employed is only a few percent, and 3) the filters operate in the high reflection limit. The last factor is important since polarization dependent reflectivity is suppressed in the high reflectivity limit. The filters are found to shift with temperature at a rate of ≈10 pm/C. The passbands of Fig. 4 exceed the 13-nm CWDM standard and the excess widths serve as guardbands sufficiently wide to make the device passively athermal over approximately 100 C.

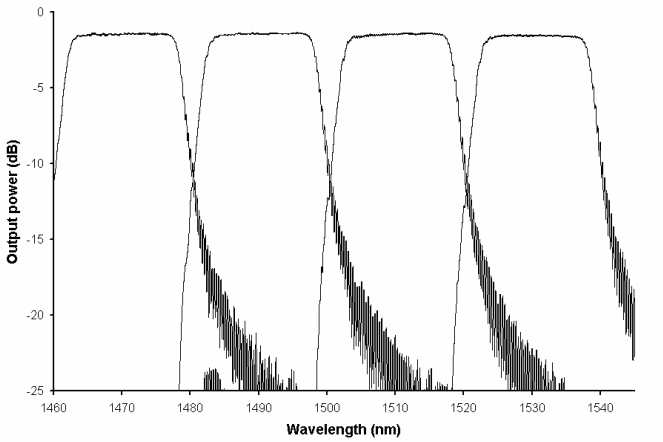

Fig. 6. Channel passbands of an unapodized (constant reflective amplitude) four channel mux. Insertion loss exhibits negligible increase with channel number.

To produce the steep passband falloff in the wings shown in Figs. 4 and 5, apodization was necessary. For comparison, a multiplexer comprised of unapodized integrated holographic filters was constructed. In the unapodized case, the contour spacing follows a linear chirp with position-independent reflection amplitude. The measured passbands of the four unapodized channels are shown in Fig. 6. (Note the bluest channel is 20 nm shorter in wavelength – an intentional shift for reasons irrelevant to the instant exposition.) As expected the passband falls off significantly more slowly in the wings. Still, unapodized devices are useful as multiplexers where channel cross-talk is less critical than in a demultiplexer. The insertion loss of the first channel of this unapodized device, 1.5 dB, is comparable to the corresponding apodized channel. However, the final channel of the apodized device has an IL about 0.5 dB higher. This may result from apodization-induced, out-of-plane scattering. We note that more advanced apodization methods, which do not induce out-of-plane scattering, are under development.

4. Summary

Monolithically integrated, single-mode-compatible, multiplexers based on integrated holographic filters have been demonstrated and found to be competitive with or superior to many existing thin-film-filter-based devices. In fact, the integrated holographic filter functions via the same principle as thin-film filters but does so in a fully integrated rather than discrete environment and incorporates signal routing function as well. Lithographically scribed, integrated holographic filtering elements may provide an important building-block element of future photonic integration.

#10401 - $15.00 USD Received 23 January 2006; revised 31 March 2006; accepted 3 April 2006